Int. J. Heat Mass Transfer. Vol. 19, pp. 413–423. Pergamon Press 1976. Printed in Great Britain

A THEORETICAL STUDY OF HEAT TRANSFER IN TWO-DIMENSIONAL TURBULENT FLOW IN A CIRCULAR PIPE AND BETWEEN PARALLEL AND DIVERGING PLATES

P. L. STEPHENSON
Central Electricity Research Laboratories, Kelvin Avenue, Leatherhead, Surrey, England

(*Received* 19 *December* 1974 *and in revised form* 27 *May* 1975)

Abstract—Developing turbulent flow and heat transfer in a circular tube and between parallel and diverging plates have been predicted by the use of a finite-difference solution procedure. A turbulence model involving the solution of partial differential equations for two turbulence quantities has been employed. Predictions have been compared with a variety of measurements and the agreement between the present predictions and published experimental results is encouraging.

NOMENCLATURE

C_μ, C_1, C_2, constants in turbulence model;
C_p, specific heat at constant pressure;
C_{f_b}, friction factor, defined on bulk velocity $\left(\frac{2\tau_w}{\rho u_b^2}\right)$;
C_{f_s}, friction factor, defined on centreline velocity $\left(\frac{2\tau_w}{\rho u_s^2}\right)$;
d_e, equivalent diameter (D or $2L$);
D, pipe diameter;
E, constant in log-law (equation 10);
h, enthalpy;
k, kinetic energy of turbulence $\left(\frac{\overline{u'^2}+\overline{v'^2}+\overline{w'^2}}{2}\right)$;
l_M, mixing-length;
L, spacing between parallel plates;
P, pressure;
$\dot{q}''_W$, wall heat flux;
r, distance from centreline of pipe;
Re_b, Reynolds number, defined on bulk velocity $\left(\frac{u_b d_e}{\nu}\right)$;
Re_s, Reynolds number, defined on centreline velocity $\left(\frac{u_s d_e}{\nu}\right)$;
St_b, Stanton number, defined on bulk enthalpy $\left(\frac{\dot{q}''_w}{\rho u_b(h_w-h_b)}\right)$;
St_i, Stanton number, defined on inlet enthalpy $\left(\frac{\dot{q}''_w}{\rho u_b(h_w-h_i)}\right)$;
T_u, turbulence intensity $\frac{1}{u_b}\sqrt{(\frac{2}{3}k)}$;
T, absolute temperature;
u, time-mean velocity in x direction;
$\overline{u'^2}$, mean square fluctuating velocity in x direction;
u_τ, friction velocity $[\sqrt{(\tau_w/\rho)}]$;
u^+, dimensionless velocity (u/u_τ);
v, time-mean velocity in r or y direction;
$\overline{v'^2}, \overline{w'^2}$, mean square fluctuating velocity in y, x directions;
x, distance along pipe or duct from inlet;
y, distance from duct or pipe centreline, perpendicular to centreline;
y^+, dimensionless distance from wall $(y_w-y)(u_\tau/\nu)$;
z, direction perpendicular to x and y.

Greek symbols

α, parameter specifying geometry (zero for plane flow, unity for axisymmetric flow);
δ, initial boundary-layer thickness;
δ^*, displacement thickness $\int_0^{y_w}\left(1-\frac{u}{u_s}\right)dy$;
ε, rate of dissipation of kinetic energy of turbulence;
θ, momentum thickness $\int_0^{y_w}\frac{u}{u_s}\left(1-\frac{u}{u_s}\right)dy$;
κ, constant in mixing-length distribution;
μ, dynamic viscosity;
ν, kinematic viscosity;
ρ, density;
σ, Prandtl/Schmidt number;
τ, shear stress.

Subscripts

b, bulk conditions;
eff, effective value;
h, enthalpy;
i, inlet value;
l, laminar;
r, reference;
s, centreline;
t, turbulent;
w, wall.

1. INTRODUCTION

THE MASS-TRANSFER analogue technique has been employed recently by Neal [1], to measure heat-transfer rates in the entrance region of a straight, circular pipe, with turbulent air flow. The experiment was arranged to provide, as nearly as possible, a uniform velocity distribution at the pipe inlet, and to ensure that the developing boundary-layer along the pipe wall was turbulent throughout its length.

This experimental work prompted the present theoretical study. An examination of the published theoretical work (Section 2.2) indicated that an algebraic turbulence model (such as a mixing-length model) would not be entirely satisfactory for this geometry. Therefore, a turbulence model involving solution of partial differential equations for the turbulence kinetic energy, k, and the rate of dissipation of kinetic energy of turbulence, ε, has been employed.

Only a limited number of detailed experimental results for developing flow in a circular pipe were found in the literature and, therefore, the present study has been extended to include turbulent developing flow between parallel and diverging plates. Throughout the present study, fluid properties are assumed to be constant.

2. PREVIOUS WORK

2.1. *Experimental studies*

Detailed hydrodynamic measurements, for developing turbulent flow in a circular pipe, have been reported by Barbin and Jones [2]. For isothermal flow at a single Reynolds number, these workers reported measurements of time-mean velocity, wall shear stress, and some turbulence quantities. Further hydrodynamic measurements have been reported by Weir *et al.* [3].

Heat-transfer measurements for a circular pipe (mostly of the variation of Stanton number) have been reported by various workers [4–9].

Recently, Neal [1] has presented values of Stanton number obtained from a mass-transfer analogue technique using naphthalene.

Detailed hydrodynamic measurements for developing flow between plates have been made by Comte-Bellot [10] and Bradshaw *et al.* [11]. Further hydrodynamic measurements, and also heat transfer measurements, have been reported by Byrne *et al.* [12], Marriott [13], and Hatton and Woolley [14]. Similar measurements, for flow and heat transfer in a straight-sided diverging duct, have been reported by Ellison [15] and O'Connor [16].

2.2. *Theoretical studies*

Integral techniques have frequently been employed in the study of developing turbulent flow. For example, Ross [17], Filippov [18] and Bowlus and Brighton [19] have applied this technique to a circular pipe, Deissler [20] and Na and Lu [21] have applied it to both circular pipes and parallel plates, and Byrne *et al.* [12] have applied it to parallel plate flow.

Other studies have entailed a finite difference solution of the governing equations, with the use of an algebraic turbulence model, such as Prandtl's mixing-length hypothesis or the Van Driest eddy diffusivity hypothesis. Such studies include those of Bankston and McEligot [22], Hutton [23], and recent studies at the Central Electricity Research Laboratories by Oliver (private communication, 1972), and have shown that algebraic turbulence models have certain limitations in developing flow. Experiments for developing flow in a pipe [2], [3] and in parallel duct [11], [12] show that the velocity profiles and turbulence structure alter significantly after the boundary-layers merge. For example, the measured centreline velocity rises to a maximum and then decays towards the fully-developed value. However, in several of the studies mentioned above, for example, [23], the centreline velocity was predicted to rise monotonically to its fully-developed value.

A turbulence model involving solution of a partial differential equation for the kinetic energy of turbulence has been applied to developing pipe and duct flow by Oliver (private communication, 1973) at the Central Electricity Research Laboratories, and by Hatton and Woolley [14]. A further model, involving a second partial differential equation (for dissipation of turbulence kinetic energy, ε) has been developed by Launder (see, for example [24]) and has been employed by Le Feuvre [25]. Both types of model predict a peak in centreline velocity in developing flow. The former type still needs algebraic equations for length scale and therefore the latter type, the k–ε model, has been employed in the present study.

Predictions for developing flow between parallel and diverging plates have been presented recently by Bradshaw *et al.* [11], based on an adaption of the boundary-layer calculation method of Bradshaw, Ferriss and Atwell [26].

3. MATHEMATICAL MODEL AND SOLUTION PROCEDURE

3.1. *Conservation equations*

The boundary-layer assumption is employed, and it is assumed, following Patankar and Spalding [27], that the equations for continuity and for conservation of momentum and enthalpy can be written as follows:

$$\frac{\partial u}{\partial x}+\frac{1}{r^\alpha}\frac{\partial}{\partial y}(r^\alpha v)=0 \tag{1}$$

$$\rho u\frac{\partial u}{\partial x}+\rho v\frac{\partial u}{\partial y}=\frac{1}{r^\alpha}\frac{\partial}{\partial y}\left(r^\alpha\mu_{\text{eff}}\frac{\partial u}{\partial y}\right)-\frac{\mathrm{d}P}{\mathrm{d}x}, \tag{2}$$

$$\rho u\frac{\partial h}{\partial x}+v\frac{\partial h}{\partial y}=\frac{1}{r^\alpha}\frac{\partial}{\partial y}\left(\frac{r^\alpha\mu_{\text{eff}}}{\sigma_{h,\text{eff}}}\cdot\frac{\partial h}{\partial y}\right), \tag{3}$$

where y and r are measured from the duct or pipe centreline (r is used only for pipe flow), and x is the distance along the pipe axis. The parameter α is zero for plane flow and unity for axisymmetric flow.

Equations (1)–(3) differ from those of Patankar and Spalding, as constant fluid properties are assumed, and effects of kinetic heating are neglected. Thus the enthalpy, h, is defined as:

$$h = C_p(T-T_r), \tag{4}$$

where T_r is a (constant) reference temperature, usually taken to be either the wall or inlet temperature.

The pressure gradient equation (2) is calculated in the way given in [27].

3.2. *Turbulence model*

A turbulence model involving solution of partial differential equations for kinetic energy of turbulence, k, and rate of dissipation of this energy, ε, has been developed by Launder and co-workers (see, for example [24, 28, 29]). The present study used the high Reynolds number form of this model [25]; the following equations are solved for k and ε;

$$\rho u \frac{\partial k}{\partial x} + \rho v \frac{\partial k}{\partial y} = \frac{1}{r^\alpha} \frac{\partial}{\partial y}\left(\frac{r^\alpha \mu_{\text{eff}}}{\sigma_k} \cdot \frac{\partial u}{\partial y}\right) + \mu_t \left(\frac{\partial u}{\partial y}\right)^2 - \rho\varepsilon \quad (5)$$

and

$$\rho u \frac{\partial \varepsilon}{\partial x} + \rho v \frac{\partial \varepsilon}{\partial y} = \frac{1}{r^\alpha} \frac{\partial}{\partial y}\left(\frac{r^\alpha \mu_{\text{eff}}}{\sigma_\varepsilon} \cdot \frac{\partial \varepsilon}{\partial y}\right) + C_1 \frac{\varepsilon}{k} \mu_t \left(\frac{\partial u}{\partial y}\right)^2 - C_2 \rho \frac{\varepsilon^2}{k}. \quad (6)$$

The turbulent and effective viscosities are defined as,

$$\mu_t = C_\mu \rho k^2/\varepsilon \quad (7)$$

and

$$\mu_{\text{eff}} = \mu_l + \mu_t. \quad (8)$$

In addition, a Couettė flow analysis, as described in [27], is used near the wall; this is based on a mixing-length defined as,

$$l_M = \kappa(y_w - y), \quad (9)$$

where y is measured from the duct centreline, and y_w is the distance from the duct centreline to the duct wall.

In the log-law based on equation (9), namely

$$u^+ = \frac{1}{\kappa} \ln y^+ + E, \quad (10)$$

the constant E is given a value of 5·5. To ensure that the k–ε model is consistent, near the wall, with a log-law based on equation (9), the various constants have to satisfy the relationship,

$$\kappa^2 = \sigma_\varepsilon (C_2 - C_1)\sqrt{(C_\mu)}. \quad (11)$$

The procedure adopted here is to specify all constants except C_1, which is then found from equation (11). For all pipe flow and some plane flow calculations, the values used are $C_\mu = 0{\cdot}09$, $C_2 = 1{\cdot}90$, $\sigma_k = 1{\cdot}0$, $\sigma_\varepsilon = 1{\cdot}0$, $\kappa = 0{\cdot}42$, giving $C_1 = 1{\cdot}13$. Other plane flow calculations have been made with $\sigma_\varepsilon = 1{\cdot}3$ (giving $C_1 = 1{\cdot}42$). These values of constants were in use at Imperial College, London, for a variety of flows, at the time of the present study.

The effective Prandtl number for enthalpy, $\sigma_{h,\text{eff}}$, is found from the expression:

$$\frac{\mu_{\text{eff}}}{\sigma_{h,\text{eff}}} = \frac{\mu_l}{\sigma_{h,l}} + \frac{1}{\sigma_{h,t}} \cdot (\mu_{\text{eff}} - \mu_l), \quad (12)$$

with the laminar Prandtl number, $\sigma_{h,l} = 0{\cdot}7$ and $\sigma_{h,t} = 0{\cdot}9$.

3.3. *Initial and boundary conditions*

At the pipe or duct inlet, a finite velocity boundary-layer thickness, δ, is assumed, together with a power-law velocity profile. Except for close to the wall, the turbulent kinetic energy, k, is assumed to vary linearly across the boundary-layer. This approximates to measurements of Klebanoff, quoted by Hinze [30]. The dissipation, ε, is calculated from k and from an assumed mixing-length distribution. The enthalpy is assumed uniform across the pipe or duct inlet.

For the earlier part of the flow, the region of integration covers only the part of the flow near the wall where significant changes occur in dependent variables. Across the central core of the flow, the dependent variables are assumed to be uniform. To find the axial variation of u, the mass flow through the portion of flow included in the region of integration is calculated. This is subtracted from the known total mass flow to find the mass flow, and thus the velocity, of the fluid in the central core. The axial variation of k and ε is found from the degenerate, free stream form of equations (5) and (6), as described in [28]. For the latter part of the calculations, one edge of the region of integration lies on the pipe or duct centreline, enabling a symmetry boundary condition to be used.

It is, of course, possible to have the region of integration extending from duct centreline to pipe walls, and to use a symmetry boundary condition through the calculations. However, the method adopted here enables sufficient cross stream grid nodes to be placed within the boundary layer, without the total number of nodes becoming excessive. Typically, the region of integration initially covers the outer 25 per cent of the pipe or duct. Also, for the node nearest the wall, the value of y^+ varies from about 75 at entry to about 130 in fully-developed flow. The grid is non-uniform, with the distance between cross-stream nodes decreasing as the wall is approached and the downstream (x direction) grid spacing is proportional to the grid width.

The boundary condition for enthalpy, h, at the wall corresponds to either a fixed wall temperature or a fixed wall heat flux. The wall boundary conditions for k and ε are derived from a Couette flow analysis, using the approach of [27]; further details are given in the Appendix.

3.4. *Solution of the equations*

The governing set of parabolic equations [equations (1–3, 5, 6)] have been solved by a modified version of the numerical procedure for boundary-layer flow developed by Patankar and Spalding [27]. For most of the calculations reported here, 30 cross stream nodes have been employed, together with a downstream step length equal to 10 per cent of the grid width. As a check on numerical accuracy, a few calculations have been made with either 40 cross stream nodes or a step length equal to 5 per cent of the grid width. In neither case were the predictions altered by more than 1 per cent.

4. RESULTS AND DISCUSSION

4.1. *Predictions for a parallel duct*

Measurements of flow and heat transfer in a parallel duct have been reported by Byrne *et al.* [12], Hatton and Woolley [14] and Marriott [13]. These workers employed a rectangular duct, 0·051 m high, 0·762 m wide and 3·66 m long, with air flow. The aspect ratio, therefore, was 15:1. The duct was preceded by a 6:1 area ratio contraction with a honeycomb, and a 0·051 m wide sandpaper strip was fixed to the duct at inlet, to ensure a turbulent boundary-layer throughout the duct. Heating started immediately after this strip, and approximated to uniform heat flux (Hatton, private communication, 1974). Although only one wall was heated, these workers derived values for two heated walls from their measurements, and presented results in this way. Therefore all results shown here are for two walls heated. The method for deriving values for two heated walls from the measurements assumed that the temperature of the unheated wall did not change, and therefore was valid only when x/L was small compared to $(St_b)^{-1}$.

The present predictions, for $Re_b = 140\,000$, are compared with measurements in Figs. 1 and 2 (the constant $\sigma_\varepsilon = 1{\cdot}0$). The calculations were based on a uniform wall heat flux, with heating starting at $x = 0{\cdot}051$ m, as the measurements approximate to this situation. The agreement between measured and predicted velocities (Fig. 1) is reasonable, except that the predicted centre-line velocity drops more rapidly from its maximum than do the measured values. Similar discrepancies exist between the measured and predicted boundary-layer thickness (Fig. 2), and may mean that the k–ε model predicts too rapid a development of the flow after the boundary-layers merge. Although it may appear from Fig. 1 that the analysis lost means going downstream, a check has shown that this was not the case.

Predictions for two values of inlet turbulence kinetic energy (namely $k_s/u_s^2 = 10^{-4}$ and 25×10^{-4}) are shown; these correspond to an inlet turbulence intensity, defined here as

$$T_u = \frac{1}{u_b} \cdot \sqrt{\left(\frac{2k}{3}\right)}, \tag{13}$$

of about 0·8 per cent and 4 per cent. Further predictions, for $k_s/u_s^2 = 1{\cdot}5 \times 10^{-6}$ (T_u about 0·1 per cent) have been found to be similar to those for $k_s/u_s^2 = 10^{-4}$. This shows that the inlet turbulence level has only a small effect on predictions, provided that k_s/u_s^2 is less

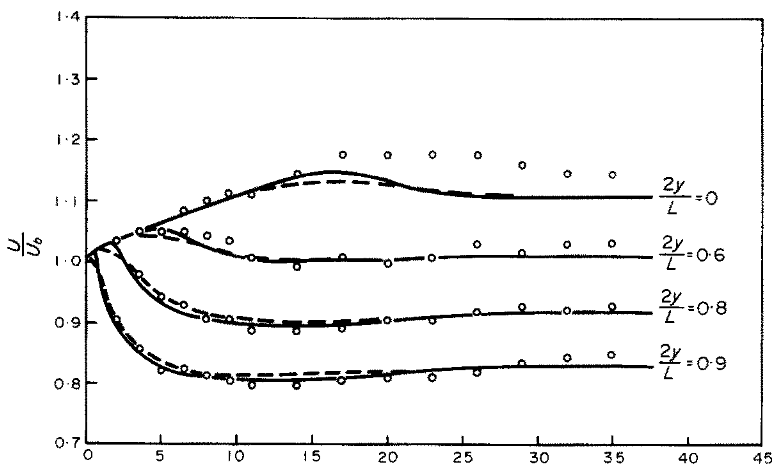

FIG. 1. Developing flow between parallel plates; variation of velocity for $Re_b = 140\,000$. ⊙, measurements, Byrne *et al.* [12]. —— predictions, for $k_s/u_s^2 = 10^{-4}$ at inlet. ---- predictions for $k_s/u_s^2 = 25 \times 10^{-4}$ at inlet.

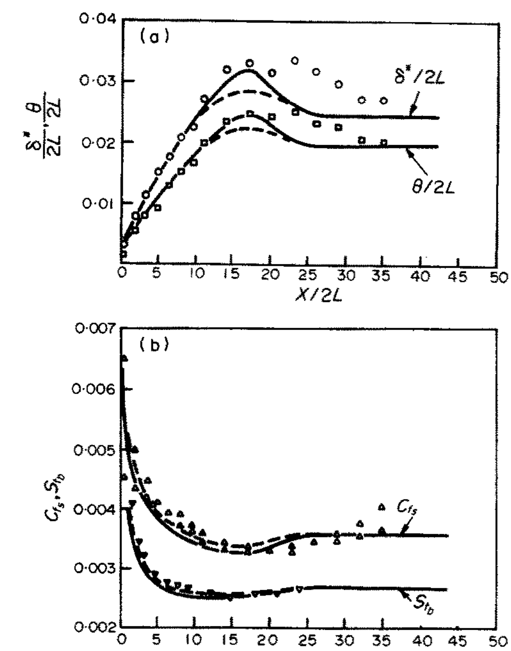

FIG. 2. Developing flow between parallel plates for $Re_b = 140\,000$: (a) variation of momentum and displacement thickness; (b) variation of friction factor and Stanton number. Measurements (Marriott [13]): ⊙, $\delta^*/2L$; ☐, $\theta/2L$; △, C_{f_s}; ▽, St_b. Predictions: —— $k_s/u_s^2 = 10^{-4}$ at inlet; ---- $k_s/u_s^2 = 25 \times 10^{-4}$ at inlet.

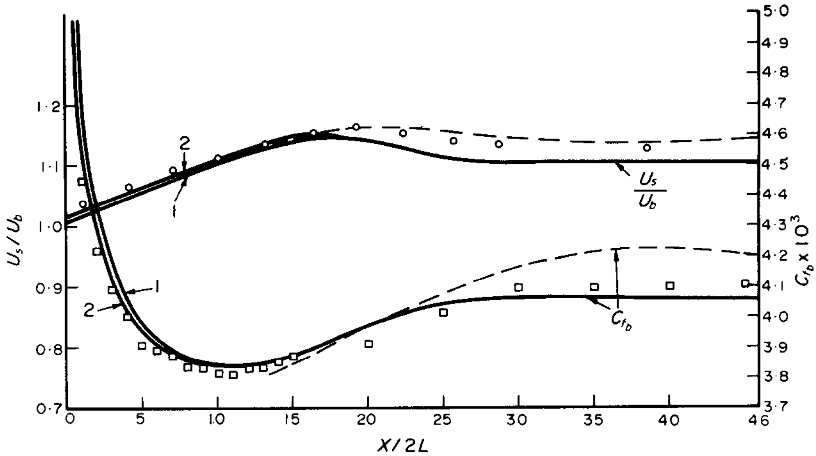

FIG. 3. Developing flow in a parallel duct; variation of centreline velocity and wall shear stress for $Re_b = 192\,000$. Measurements (Bradshaw *et al.* [11]): ○, u_s/u_b; □, C_{f_b}. Predictions: —— present study; (1), $\delta/L = 0.025$ at inlet; (2), $\delta/L = 0.040$ at inlet; ---- Bradshaw *et al.* [11].

than about 10^{-4}. A higher inlet turbulence level gives higher values of effective viscosity near the boundary-layer edge; thus values of C_{fb} and St_b are increased, and the values of u_s, δ^* and θ overshoot their fully-developed values to a lesser extent.

Measurements for isothermal air flow in a parallel wall duct have been reported by Bradshaw *et al.* [11]. The duct was 0·05 m by 0·61 m (nominal), and was preceded by a 12:1 contraction and honeycomb (Bradshaw, private communication, 1974). The turbulence intensity at inlet was less than 0·1 per cent, and the boundary-layer was tripped by wires approximately 1 mm in diameter, at the downstream end of the contraction.

The present predictions have been made for $Re_b = 192\,000$, and are compared with measurements in Fig. 3. The calculations are for $\sigma_\varepsilon = 1{\cdot}0$, for an inlet turbulence kinetic energy of $k_s/u_s^2 = 1{\cdot}5 \times 10^{-6}$, and for two values of inlet boundary-layer thickness δ (namely $\delta/L = 0{\cdot}025$ and 0·04). The diameter of the trip wire used in the experiments was about $0{\cdot}02L$, so these are plausible initial boundary-layer thicknesses. The greater inlet boundary-layer thickness naturally gives a higher inlet value of u_s/u_b. It also gives lower velocity gradients and shear stresses, and thus lower values of C_{f_b}. Further calculations have been made for $\sigma_\varepsilon = 1{\cdot}3$ and have yielded results similar to those here.

Predictions of Bradshaw, Dean and McEligot [11] are also included in Fig. 3; these predictions, based on an adaption of the boundary-layer approach of Bradshaw *et al.* [26], and were started just upstream of the point where the boundary-layers merge. These results agree well with both measurements and the present predictions; the large scale of Fig. 3 exaggerates small differences.

The predicted fully-developed profiles for u and k are compared with measurements [10, 31, 32] in Fig. 4. The comparatively small effect on the k profile of altering σ_ε from 1·0 to 1·3 is also shown in Fig. 4; the effect on u of altering σ_ε was even less. Increasing σ_ε

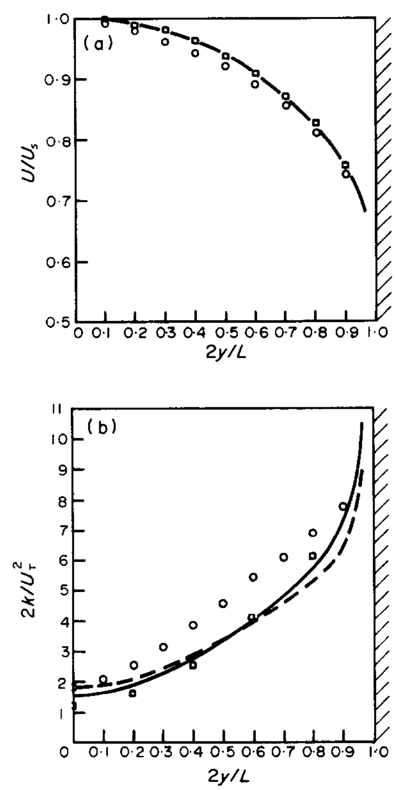

FIG. 4. Fully-developed flow between parellel plates. (a) Fully-developed velocity profile. ⊡, measurement, Schlicting [31]; ⊙, measurement, Comte-Bellot [10], $Re_b = 228\,000$; —— prediction, for $Re_b = 192\,000$ and $\sigma_\varepsilon = 1.0$. (b) Fully-developed turbulence kinetic energy profile. ⊡, measurement, Clarke [32], for $Re_s = 110\,000$; ⊙, measurement, Comte-Bellot [10], for $Re_b = 228\,000$; —— prediction, for $Re_b = 192\,000$ and $\sigma_\varepsilon = 1.0$; ---- prediction, for $Re_b = 192\,000$ and $\sigma_\varepsilon = 1.3$.

reduced diffusion of ε away from the wall, making ε higher near the wall and lower elsewhere. Thus k is lower near the wall and higher elsewhere.

The predicted values of C_{f_b} and St_b in fully-developed

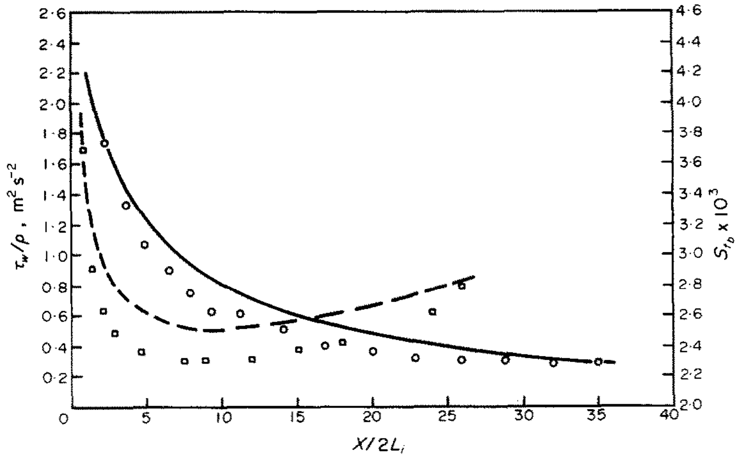

FIG. 5. Developing flow in a diverging duct; wall shear stress and Stanton number for $Re_b = 206800$. Measurement (Hatton, Woolley [14]); ⊙, τ_w/ρ; ⊡, $St_b \times 10^3$. Prediction; —— τ_w/ρ; ---- $St_b \times 10^3$; (heat-transfer results for constant wall heat flux).

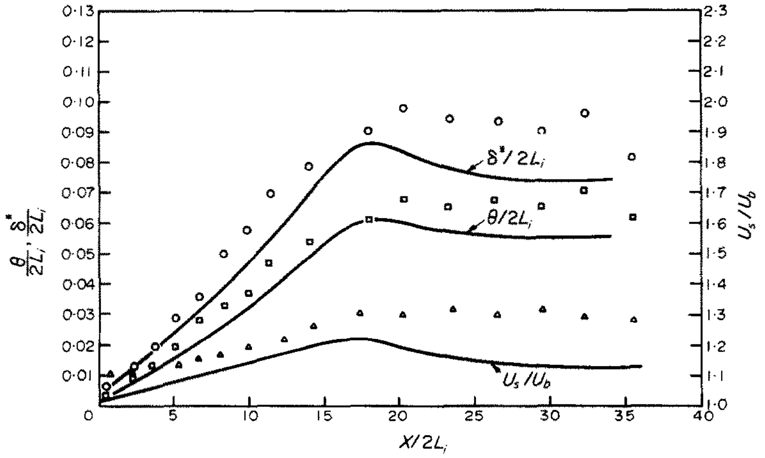

FIG. 6. Developing flow in a diverging duct; momentum and displacement thickness and centreline velocity, for $Re_b = 206800$. Measurement (Hatton, Woolley [14]): ○, $\delta^*/2L_i$; ⊡, $\theta/2L_i$; △, u_s/u_b. Prediction ——.

Table 1. Comparison of values of friction factor and Stanton number in fully-developed flow

Geometry	Details	$C_{f_b} \times 10^3$	$St_b \times 10^3$
Parallel duct	Correlation [33]	3·94	2·54
($Re_b = 192000$)	Prediction, $\sigma_\varepsilon = 1{\cdot}0$	4·13	2·47
	Prediction, $\sigma_\varepsilon = 1{\cdot}3$	4·05	2·39
Circular pipe	Correlation [33]	3·43	—
($Re_b = 388000$)	Correlation [33]	—	2·10
	Prediction, $\sigma_\varepsilon = 1{\cdot}0$	3·45	2·00

flow with $Re_b = 192000$ are compared in Table 1 with values calculated from the following correlations, which are recommended by Knudsen and Katz [33];

$$C_{f_b}^{-\frac{1}{2}} = 4{\cdot}0\log_{10}[Re_b\sqrt{(C_{f_b})}] - 0{\cdot}40, \quad (14)$$

and

$$St_b = 0{\cdot}023Re_b^{-0{\cdot}2}Pr^{-2/3}. \quad (15)$$

4.2. *Predictions for a diverging duct*

Measurements of flow and heat transfer in a diverging duct have been reported by Ellison [15], O'Connor [16] and Hatton and Woolley [14]. These workers employed a duct of rectangular cross section, 3·66 m long and 0·82 m wide. The gap width varied from 0·05 m at inlet to 0·152 m at exit. The side walls of the duct were given a slight spanwise divergence (that is, in a direction perpendicular to x and y), in order to provide a two-dimensional flow. However, there is some evidence [15] that three-dimensional effects became significant towards the end of the duct. The experimental rig was similar to that of Marriott [13]; a sandpaper strip, 0·051 m wide, was placed at the duct inlet, to trip the boundary-layers. Also, the lower side only was heated (with an element starting immediately after the sandpaper strip) and results for two sides heated were calculated by these workers from their measurements. The turbulence intensity at inlet was about 0·6 per cent.

The present predictions, for $Re_b = 206800$, are compared with measurements in Fig. 5 and 6. The calculations have been made for $k_s/u_s^2 = 10^{-4}$ and $\delta/L_i = 0{\cdot}025$ at inlet and with $\sigma_\varepsilon = 1{\cdot}0$. The thermal boundary condition was the same as in Section 4.1. The agreement between measured and predicted values of τ_w (Fig. 5) is reasonable; however, the minimum predicted value of

St_b is significantly higher than the corresponding measured value. This discrepancy may be caused in part by experimental errors; values for a duct for two sides heated were derived by Hatton and co-workers from measurements for a duct with one side heated, and there may be significant three-dimensional effects. Also, the inlet boundary-layer thickness and turbulence intensity are not known accurately, and predictions for a parallel duct (Figs. 2, 3) show that these parameters can affect the minimum predicted value of St_b. The reasonable agreement between measured and predicted values of momentum and displacement thickness (Fig. 6) suggests that a correct initial boundary-layer thickness was employed in the calculations. Therefore, the discrepancies between measured and predicted values of u_s/u_b near the duct inlet may be due to a systematic error in the measurements.

4.3. *Predictions for a circular pipe*

Detailed hydrodynamic measurements for developing flow in a circular pipe have been presented by Barbin and Jones [2]. They employed a 0·203 m diameter pipe, preceded by a bellmouth contraction, and with a 1-in strip of sandpaper grains fixed near the inlet to trip the boundary-layer.

The present predictions, for $Re_b = 388\,000$ are compared with measurements in Fig. 7 and 8. Fully-developed velocity ratios from the universal velocity defect law (Schlicting [31]) are included in Fig. 8. The calculations are for $k_s/u_s^2 = 10^{-4}$ and $\delta/D = 0{\cdot}0125$ at inlet, and $\sigma_\varepsilon = 1{\cdot}0$. The measurements shown in Fig. 7(a) were presented by Barbin and Jones as values of wall shear stress; however, their measurements should probably be regarded as values of pressure gradient [12]. Results are shown in Fig. 7(a) as the ratio of local to fully-developed value, as Barbin and Jones [2] presented their results in this way. However, it can be seen from Table 1 that the agreement between measured and predicted absolute values of C_{f_b} (and hence τ_w and dp/dx) is satisfactory in fully-developed flow.

The pipe employed by Barbin and Jones [2] was probably not sufficiently long to produce fully-developed flow, and therefore the peak in centreline velocity is not entirely clear in their measurements (see Fig. 8). However, more recent measurements by Weir *et al.* [3] for $Re_b = 425\,000$, show a pronounced peak in centreline velocity, with u_s/u_b having a maximum

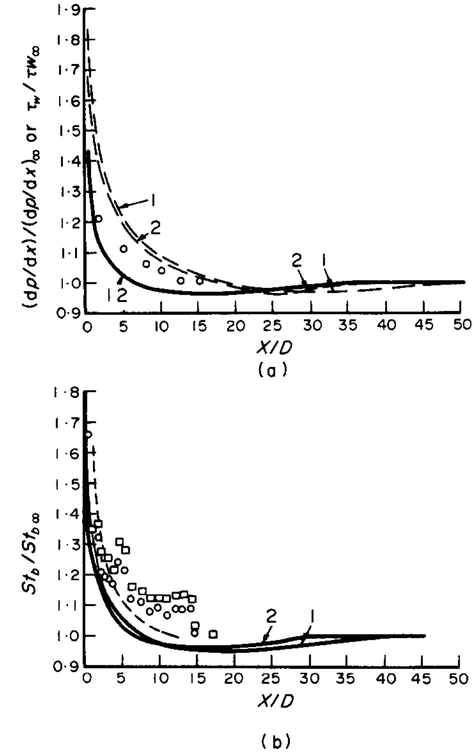

FIG. 7. Developing flow in a circular tube. (a) variation of wall shear stress and pressure gradient for $Re_b = 388\,000$. Measurement (Barbin, Jones [2]); ⊙, $(dP/dx)/(dP/dx)_\infty$; Predictions: ——, τ/τ_∞; ----, $(dP/dx)/(dP/dx)_\infty$; (1) k–ε model; (2) mixing-length model: (b) variation of Stanton number. Measurements (Boelter *et al.* [5]): ⊙, bell mouth only, for $Re_b = 55\,570$; ⊡, bell mouth and one grid, for $Re_b = 55\,570$. Measurements (Mills [7]), for $Re_b = 78\,700$, ----. Predictions, for $Re_b = 388\,000$ ——; (1), k–ε model; (2) mixing-length model.

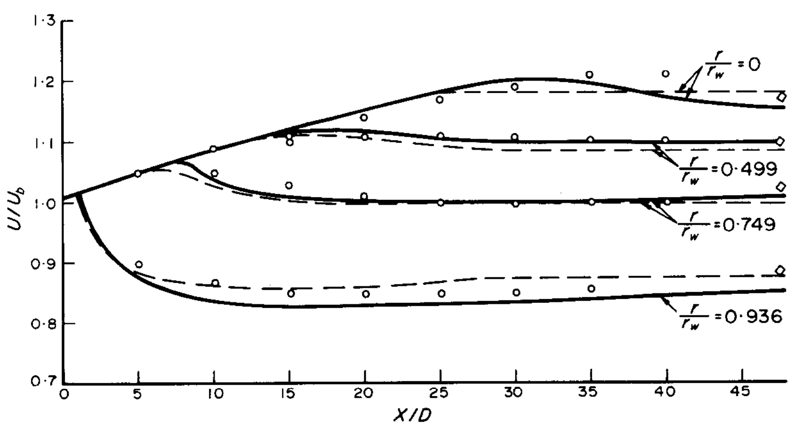

FIG. 8. Developing flow in a circular tube; variations of velocity for $Re_b = 388\,000$. ⊙, measurements (Barbin and Jones [2]), for same radius ratios and predictions; ◇, fully-developed values, from universal velocity defect law, for same radius ratios as predictions; ——, predictions for k–ε model; ----, predictions for mixing-length model.

value of 1·23 at x/D of about 40. Also, the fully developed value of u_s/u_b was not reached until x/D was between 60 and 70.

Predictions of Stanton number are shown in Fig. 7(b), and correspond to the hydrodynamic results shown in Fig. 7(a) and 8. They are for uniform wall temperature, as the measurements of Neal [1], correspond to this boundary condition. No measurements of Stanton number for this Reynolds number and boundary condition have been found in the literature. However, it has been found experimentally [7, 8] and confirmed in the present study, that neither the Reynolds number nor the thermal boundary condition has a significant effect on the ratio of local to fully-developed Stanton number. Therefore, measurements for a uniform heat flux that have been reported by Boelter *et al.* [5] for $Re_b = 55\,570$ and by Mills [7] for $Re_b = 76\,000$ are included in Fig. 7(b). The results are expressed as the ratio of local to fully-developed Stanton number, to enable values for different Re and thermal boundary condition to be compared. However, it can be seen from Table 1 that agreement between measured and predicted values of St is satisfactory in fully-developed flow. Comparison with results of a mass-transfer analogue is deferred to Section 4.4 for convenience.

In earlier studies at the Central Electricity Research Laboratories, a mixing-length model was used to predict developing flow in a circular pipe. These calculations have been repeated, using the same constants as are used here for the k–ε near the wall (see Section 3.2). The mixing-length was limited to a maximum value of λ times the local boundary-layer width, with $\lambda = 0{\cdot}1$. This value of λ was chosen to make the predicted values of C_f and St in fully-developed flow agree with those found from correlations [see equations (16, 17)]. These mixing-length predictions are included in Figs. 7 and 8; the values of τ_w, dp/dx and St_b found from the mixing-length approach their fully-developed values faster than those found from the k–ε model. Apart from this, the two sets of predictions are similar. Greater differences occur in the velocity predictions (Fig. 8); the mixing-length predictions show no peak in centreline velocity, and no change in velocities after 25 and 30 diameters.

Predictions of fully-developed profiles for k and u are compared with measurements of Nikuradse (see [31]) and Laufer [34] in Fig. 9.

The fully-developed values of C_{f_b} and St_b are compared in Table 1 with values obtained from the correlation of Drew, Koo and McAdams (see [33]), namely:

$$C_{f_b} = 0{\cdot}00140 + 0{\cdot}125 Re_b^{-0{\cdot}32} \tag{16}$$

and that of Dittus and Boelter (see [33]), namely:

$$St_b = 0{\cdot}023 Re_b^{-0{\cdot}2} Pr^{-0{\cdot}6}. \tag{17}$$

4.4. *Comparison with mass-transfer analogue measurements*

Neal [1] employed a mass-transfer analogue technique (using naphthalene) to obtain heat-transfer measurements (Section 1). Certain difficulties were found in measuring bulk properties, and therefore Neal chose to employ the following definition of Stanton number;

$$St_i = \frac{q_w''}{\rho u_b (h_w - h_i)}, \tag{18}$$

rather than the more common definition,

$$St_b = \frac{q_w''}{\rho u_b (h_w - h_b)}, \tag{19}$$

used so far.

Measurements of Neal for $Re_b = 326\,000$ are compared with predictions for the k–ε model in Fig. 10. Predictions for the mixing-length model mentioned in Section 4.3 are included in Fig. 10, for comparison.

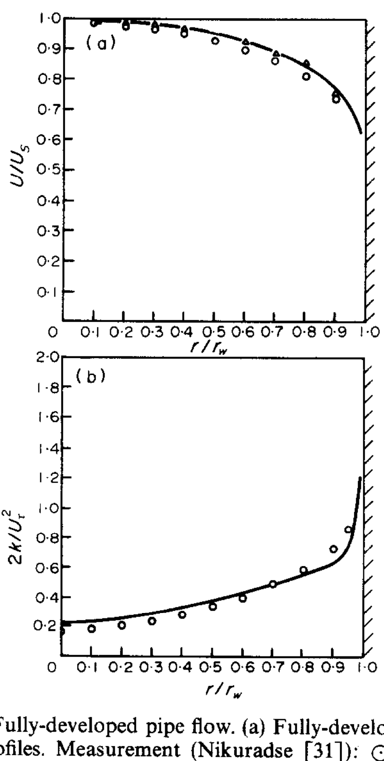

FIG. 9. Fully-developed pipe flow. (a) Fully-developed velocity profiles. Measurement (Nikuradse [31]): ⊙, $Re_b = 110\,000$; △, $Re_b = 1\,100\,000$. Prediction, $Re_b = 388\,000$: ——; (b) fully-developed kinetic energy profile. Measurement (Laufer [34]), $Re_s = 500\,000$: ⊙, Prediction, $Re_b = 388\,000$ and $x/D = 79$: ——.

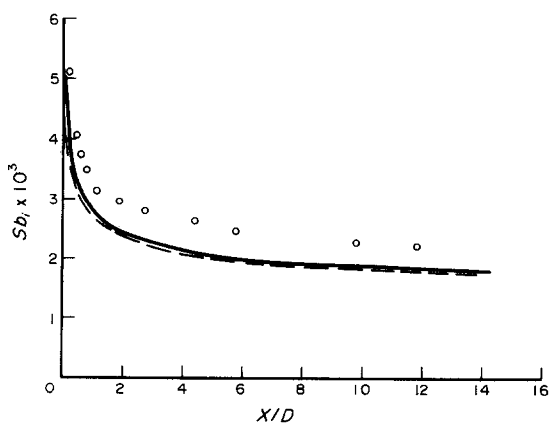

FIG. 10. Developing pipe flow; comparison with mass-transfer analogue measurements for $Re_b = 326\,000$: ⊙, measurements, Neal [1]; ——, prediction, for k–ε model; ----, prediction, for mixing-length model.

4.5. *Discussion*

4.5.1 *Use of* k–ε *model for developing flow.* The present predictions for the k–ε model are a significant improvement on earlier calculations for a mixing-length model, in that significant changes are allowed to occur after the boundary-layers merge. For instance, the peaks in centreline velocity and also in δ and θ^* can be predicted with the k–ε model. The only significant shortcoming of the k–ε predictions is that the centreline velocity and the momentum and displacement thicknesses after their maxima drop faster than the measured values (Figs. 1–3). Therefore, although it is possible to obtain reasonable predictions of C_{f_b} and St_b using a mixing-length model, a more complex model, such as the k–ε model, is required to predict the detailed features of the flow.

The present predictions exhibit minima in C_{f_b} and St_b for developing flow in a pipe or parallel plate. Unfortunately, it is not clear from the literature whether such minima occur. One difficulty is the comparatively small variations that are found in the present study; the values of C_{f_b} and St_b never drop below 90 per cent of the fully-developed values. Also, the variation of C_{f_b} and St_b may depend on such parameters as inlet turbulence level and method used to trip the boundary-layer, and these parameters vary between experimental studies. This point has been investigated by Weir *et al.* [3].

The only detailed hydrodynamic measurements for pipe flow that have been found in the literature are those of [2]; for reasons given in Section 4.3, the friction factor results of that study may be in error. Also, none of the St_b measurements found for pipe flow shows a minimum. However, the parallel duct measurements of Marriott [13], and Bradshaw *et al.* [11] show distinct minima in C_{f_b}, and the measurements of Marriott also show minima in St_b. Thus, although more detailed experimental results are desirable, and the existence of a minimum in duct flow does not necessarily imply a minimum in pipe flow, it would appear that the k–ε model is correct in predicting these minima.

The k–ε model has given reasonably successful predictions for the hydrodynamic aspects of developing flow in a two-dimensional diverging duct, although the corresponding heat-transfer predictions were not entirely satisfactory.

As a result of all the comparisons between prediction and experiment reported in this section, it is concluded that the k–ε model employed here yields reasonable predictions for developing, two-dimensional, confined turbulent flow.

4.5.2 *Comparison with mass-transfer analogue measurements.* The present predictions have been found to be in reasonable agreement with the measurements for a mass-transfer analogue experiment (Fig. 10).

The present calculations do suggest that Neal could not measure accurately the fully-developed values of Stanton number. This is partly because fully-developed conditions are probably not reached in the length of duct employed by him, and partly because a Stanton number defined as St_i does not reach a steady value in fully-developed flow.

Despite these points, the present predictions are seen to be in satisfactory agreement with the measurements of Neal.

5. CONCLUSIONS

1. The computing procedure of Patankar and Spalding [27] has been used successfully with the k–ε turbulence model developed by Launder to predict developing turbulent flow and heat transfer in a circular pipe, and between parallel plates. Successful hydrodynamic predictions have also been obtained for a diverging duct.

2. On the basis of comparison with a range of experimental results, the k–ε turbulence model used here is found to give reasonable predictions of developing flow, including detailed features that earlier studies, based on a mixing-length model, failed to predict.

3. Predictions have been obtained which are in satisfactory agreement with measurements obtained by Neal from a mass-transfer analogue technique.

Acknowledgements—This work was carried out at the Central Electricity Research Laboratories and it is published by permission of the Central Electricity Generating Board. The author also wishes to acknowledge helpful discussions with Dr B. E. Launder of Imperial College, London and Mr T. H. Massey and Mr A. J. Oliver of the Central Electricity Research Laboratories.

REFERENCES

1. S. B. H. C. Neal, The development of the thin-film naphthalene mass-transfer analogue technique for the direct measurement of heat transfer coefficients, *Int. J. Heat Mass Transfer* **18**, 559 (1975).
2. A. R. Barbin and J. B. Jones, Turbulent flow in the inlet region of a smooth pipe, *J. Basic Engng* **85**(1), 29 (1963).
3. J. Weir, A. J. Priest and V. K. Sharan, The effect of inlet disturbances on turbulent pipe flow, *J. Mech. Engng Sci.* **16**(3), 211 (1974).
4. A. Cholette, Heat transfer—local and average coefficients for air flowing inside tubes, *Chem. Engng Prog.* **44**(1), 81 (1948).
5. L. M. K. Boelter, G. Young and H. W. Iversen, Investigation of aircraft heaters—XXVII. Distribution of heat transfer rate in entrance section of a circular tube, NACA TM 1451 (1948).
6. I. T. Aladyev, Experimental determination of local and mean coefficients of heat transfer for turbulent flow in pipes, NACA TM 1356 (1954).
7. A. F. Mills, Experimental investigation of turbulent heat transfer in the entrance region of a circular conduit, *J. Mech. Engng Sci.* **4**(1), 63 (1962).
8. W. B. Hall and S. A. Khan, Experimental investigation into the effect of the thermal boundary condition on heat transfer in the entrance region of a pipe, *J. Mech. Engng Sci.* **6**(3), 250 (1964).
9. N. A. Aleksandrov, The effect of inlet conditions on heat transfer in the inlet section of a circular tube, *Thermal Engng* **10**, 103 (1971).
10. G. Comte-Bellot, Ecoulement turbulent entre deux parois parallèles, Publications Scientifique et Technique Du Ministère de l'Air, No. 419 (1965).
11. P. Bradshaw, R. B. Dean and D. M. McEligot, Calculation of interacting turbulent shear layers: duct flow, *J. Fluid Engng* **95**(2), 214 (1973).
12. J. Byrne, A. P. Hatton and P. Marriott, Turbulent flow in the entrance region of a parallel wall passage, *Proc. Instn. Mech. Engng* **184**, 697 (1969–70).
13. P. G. Marriott, Heat transfer in the entrance region of

a parallel wall passage, M.Sc. Thesis, Univ. Manchester (1969).
14. A. P. Hatton and N. H. Woolley, Heat transfer in two-dimensional turbulent confined flows, *Heat Fluid Flow* 3(1), 13 (1973).
15. G. M. Ellison, Flow and heat transfer in a straight-sided diffuser, M.Sc. Thesis, Univ. Manchester (1970).
16. J. P. O'Connor, Flow and heat transfer in rectangular, diverging ducts, M.Sc. Thesis, Univ. Manchester (1972).
17. D. Ross, Turbulent flow in the entrance region of a pipe, *Trans. Am. Soc. Mech. Engrs* **78**, 915 (1956).
18. G. V. Filippov, On turbulent flow in the entrance length of a straight tube of circular cross-section, *Soviet Phys.-Tech. Phys.* **32**(8), 1681 (1958).
19. D. A. Bowlus and J. A. Brighton, Incompressible turbulent flow in the inlet region of a pipe, *J. Basic Engng* **90**(3), 431 (1968).
20. R. G. Deissler, Turbulent heat transfer and friction in the entrance region of smooth passages, *Trans. Am. Soc. Mech. Engrs* **77**, 1221 (1955).
21. T. Y. Na and Y. P. Lu, Turbulent flow development characteristics in channel inlets, *Appl. Scient. Res.* **27**, 425 (1973).
22. C. A. Bankston and D. M. McEligot, Turbulent and laminar transfer to gases with varying properties in the entry region of circular ducts, *Int. J. Heat Mass Transfer* **13**, 319 (1970).
23. A. G. Hutton, A finite difference method for analysing the flow in the entrance region of a duct, M.Sc. Thesis, Dept. of Mech. Engng, Univ. Wales, Swansea (1971).
24. B. E. Launder and D. B. Spalding, *Mathematical Models of Turbulence*. Academic Press, New York (1972).
25. R. F. Le Feuvre, Laminar and turbulent forced convection processes through in-line tube banks, Imp. Coll. Mech. Eng. Dept. Tech. Note HTS/75.
26. P. Bradshaw, D. H. Ferriss and N. P. Atwell, Calculation of boundary layer development using the turbulent energy equation, *J. Fluid Mech.* **28**, 593 (1967).
27. S. V. Patankar and D. B. Spalding, *Heat and Mass Transfer in Boundary-Layers*, 2nd edn. International Text Book, London (1970).
28. W. P. Jones and B. E. Launder, The prediction of laminarization with a two equation model of turbulence, *Int. J. Heat Mass Transfer* **15**, 301 (1972).
29. W. P. Jones and B. E. Launder, The calculation of low Reynolds-number phenomena with a two-equation model of turbulence, *Int. J. Heat Mass Transfer* **16**, 1119 (1973).
30. G. O. Hinze, *Turbulence*. McGraw-Hill, New York (1959).
31. H. Schlicting, *Boundary-Layer Theory*. McGraw-Hill, New York (1955).
32. J. A. Clarke, A study of incompressible turbulent boundary layers in channel flow, *J. Basic Engng* **90**(4), 455 (1968).
33. J. G. Knudsen and D. L. Katz, *Fluid Dynamics and Heat Transfer*. McGraw-Hill, New York (1958).
34. J. Laufer, The structure of turbulence of fully-developed pipe flow, N.A.C.A. Report 1174 (1954).

APPENDIX

Wall Boundary Conditions for k *and* ε

As the high Reynolds number form of the k–ε model is used here, the Couette flow analysis, which applies from the wall to a point half way between the wall and the first interior node, must reach into the fully turbulent part of the boundary layer. Then the equations for k and ε at the outer edge of the Couette flow region are derived from the following approach. Radius effects are neglected, so that the results apply to both plane and axisymmetric flow.

The Couette flow form of the momentum equation (equation 2) can be written as follows:

$$\frac{\mathrm{d}\tau}{\mathrm{d}y}+\frac{\mathrm{d}P}{\mathrm{d}x}=0. \tag{A.1}$$

Integrating and inserting the wall boundary condition gives the result:

$$\tau-\tau_w=\frac{\mathrm{d}P}{\mathrm{d}x}(y_w-y). \tag{A.2}$$

It is now assumed that:

$$\tau = C_\mu^{\frac{1}{2}}\rho k. \tag{A.3}$$

Combining equations (A.2) and (A.3) gives the following expression for k:

$$k=\frac{1}{\rho C_\mu^{\frac{1}{2}}}\left\{\tau_w+(y_w-y)\frac{\mathrm{d}P}{\mathrm{d}x}\right\}. \tag{A.4}$$

The dissipation, ε, is obtained from equation (A.4) and the mixing-length distribution of equation (9); the resulting expression is as follows:

$$\varepsilon=\frac{1}{k\rho^{3/2}(y_w-y)}\left\{\tau_w+(y_w-y)\frac{\mathrm{d}P}{\mathrm{d}x}\right\}^{3/2}. \tag{A.5}$$

ETUDE THEORIQUE DU TRANSFERT DE CHALEUR EN ECOULEMENT TURBULENT BIDIMENSIONNEL DANS UN TUBE CIRCULAIRE ET ENTRE DES PLAQUES PARALLELES OU DIVERGENTES

Résumé—L'écoulement et le transfert thermique turbulents non établis, dans un tube circulaire et entre plaques parallèles ou divergentes, a été évalué à l'aide d'une méthode numérique de différences finies. On a utilisé un modèle de turbulence nécessitant la résolution d'équations aux dérivées partielles pour deux quantités turbulentes. Les prévisions numériques ont été comparées à diverses mesures expérimentales et l'accord entre les présentes prévisions et les résultats publiés a été trouvé encourageant.

EINE THEORETISCHE UNTERSUCHUNG DES WÄRMEÜBERGANGS FÜR ZWEIDIMENSIONALE TURBULENTE STRÖMUNG IN EINEM KREISROHR UND ZWISCHEN PARALLELEN UND DIVERGIERENDEN PLATTEN

Zusammenfassung—Mit Hilfe der Methode finiter Elemente wurde die Ausbildung der turbulenten Strömung und des Wärmeübergangs in einem Kreisrohr und zwischen parallelen und divergierenden Platten berechnet. Ein Turbulenzmodell, das die Lösung partieller Differentialgleichungen einschließt, wurde für zwei Turbulenzgrade herangezogen. Die berechneten Werte wurden mit einer Vielzahl von gemessenen Werten verglichen und die Übereinstimmung ist ermutigend.

ТЕОРЕТИЧЕСКОЕ ИССЛЕДОВАНИЕ ПЕРЕНОСА ТЕПЛА В ДВУМЕРНОМ ТУРБУЛЕНТНОМ ПОТОКЕ, ПРОТЕКАЮЩЕМ В ТРУБЕ КРУГЛОГО СЕЧЕНИЯ, И МЕЖДУ ПАРАЛЛЕЛЬНЫМИ И РАСХОДЯЩИМИСЯ ПЛАСТИНАМИ

Аннотация — Развивающееся турбулентное течение и теплообмен в трубе круглого сечения, а также между параллельными и расходящимися пластинами рассчитывались с помощью метода конечных разностей. Использовалась модель турбулентности, включающая решение дифференциальных уравнений в частных производных для двух характеристик турбулентности. Расчеты сравнивались с рядом измерений. Соответствие между результатами, полученными и опубликованными, довольно хорошее.